Univerza v Ljubljani
Institut "Jožef Stefan" , Ljubljana
61 111 Ljubljana, Jamova 39, pp 100 / Tel:+386 61 177 3900 / Fax: +386 61 125 7074

IJS Report
IJS - DP - 7819
December 1997

An Iterative Method for the Analysis of Čerenkov Rings

P. Križan and M. Starič
Faculty of Mathematics and Physics, University of Ljubljana, and
"J. Stefan" Institute, Ljubljana, Slovenia

DRAFT

x

Abstract

A new method is presented for the analysis of data recorded with a Ring Imaging Čerenkov (RICH) counter. The method is particularly useful for events where rings overlap considerably. The algorithm was tested on simulated data for the HERA-B experiment, and its performance is compared with a maximum likelihood analysis.

1 Introduction

In the analysis of data recorded by a RICH counter one is confronted with the fact that in principle each hit on the photon detector has to be considered when the Čerenkov angle for a given charged track is being evaluated. In cases where the ring radia are rather large and track density is high, a considerable overlap of rings is possible. In such a case, the peak in the Čerenkov angle distribution corresponding to the photons from the considered track might become considerably obscured by the contribution of photons from the neighbouring tracks. In the standard approach one estimates the form of background at a given photon detector part, and calculates the likelihood functions for various particle hypotheses [1].

There certainly is room for improvement of this method. In particular, the circumstance that most of the background hits actually belong to other tracks in the event, suggests that some kind of iterative procedure, in which each photon would gradually become predominately associated with one of the tracks, could reduce the background level. One of the possible methods how to proceed in this case, is described in this contribution. Let us note that a similar method, known as expectation–maximization algorithm, is used for image reconstruction in positron emission tomography.

In what follows, we shall first present the method on a simple example of three overlapping rings, and then study the influence of a superimposed uniformly distributed background. In the next section, an appropriate maximum likelihood function will be constructed. Finally, the performance of the method will be discussed on the simulated data for the HERA-B experiment.

2 The iterative method

We shall now illustrate how the method works on a simple example of three overlapping rings, displayed in Fig. 1. For each of the tracks and for each of the photons we first calculate the corresponding ring radius, and fill a histogram shown in Fig. 2. Here the usual method, a maximum likelihood analysis of RICH data [1], would calculate the likelihood for each particle hypothesis. In our iterative approach we continue, however, to clear up the histograms. We proceed in the following way: instead of putting a given photon in all the three histograms with weight one, as we did in the first step, we ascribe weights to each photon so that the sum of weights is equal to one for each photon. The weight for a specific photon in the histogram corresponding to the track i is calculated for the next iteration according to the formula

$$w_i = \frac{y_i}{y_1 + y_2 + y_3},$$

where y_1, y_2 and y_3 is the number of entries in the bin, into which the given photon fits, in histograms 1, 2 and 3, respectively. As a result, a given photon is given the highest weight in the histogram, where it fits into a peak, and lowest, where it is part of a scarcely populated background. In the next iterations the procedure is repeated, and the resulting histograms after sixteen iterations are shown in the lower row of Fig. 2.

A closer inspection shows that the distribution of photons remains Gaussian with the same r.m.s width. Also, the number of photons in the peak, n_r ($n_r = \sum w_i$, sum of weights within $\pm 3\sigma$), remains the same (or is only slightly reduced) if compared with the input (Fig. 3). The variation in the number of photons is, however, larger than the Poissonian value because of correlations between weights w_i (Fig. 4.

This last point needs a further study, since the correct knowledge of the expected distributions is essential for the proper evaluation of the likelihood function. From Fig. 4 we conclude that the width of the distribution only slightly exceeds the expected value for small numbers of expected photons (and thus rings with a small radius), while the difference becomes significant in the case more photons are expected and the rings get larger. For the

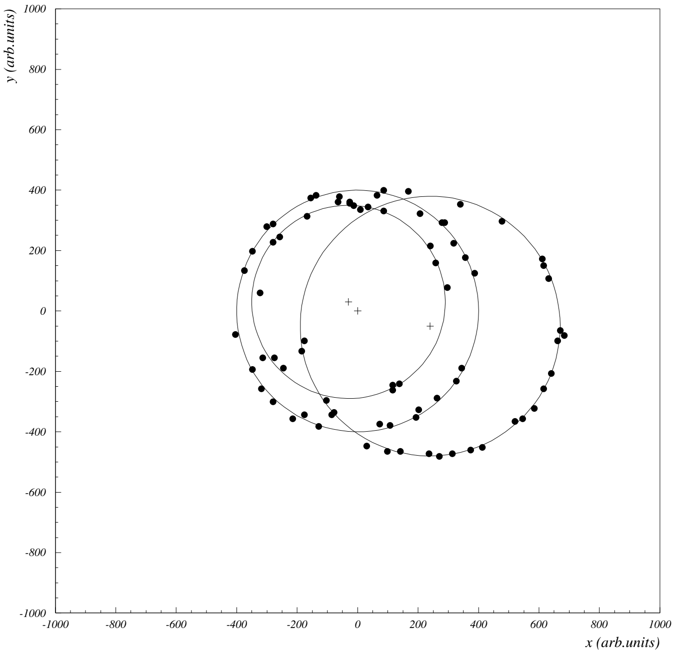

Figure 1: *The test example: three overlapping Čerenkov rings.*

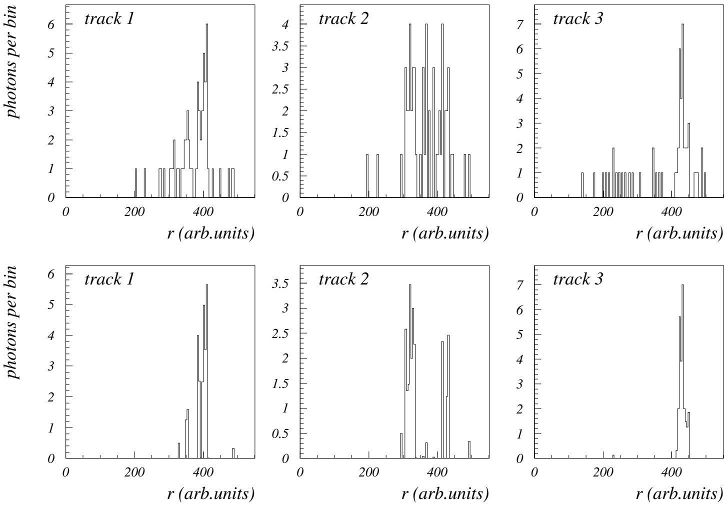

Figure 2: *Photon hit histogram for tracks 1, 2 and 3, from left to right, at the beginning of the iteration procedure (top row) and after 16 iterations (bottom).*

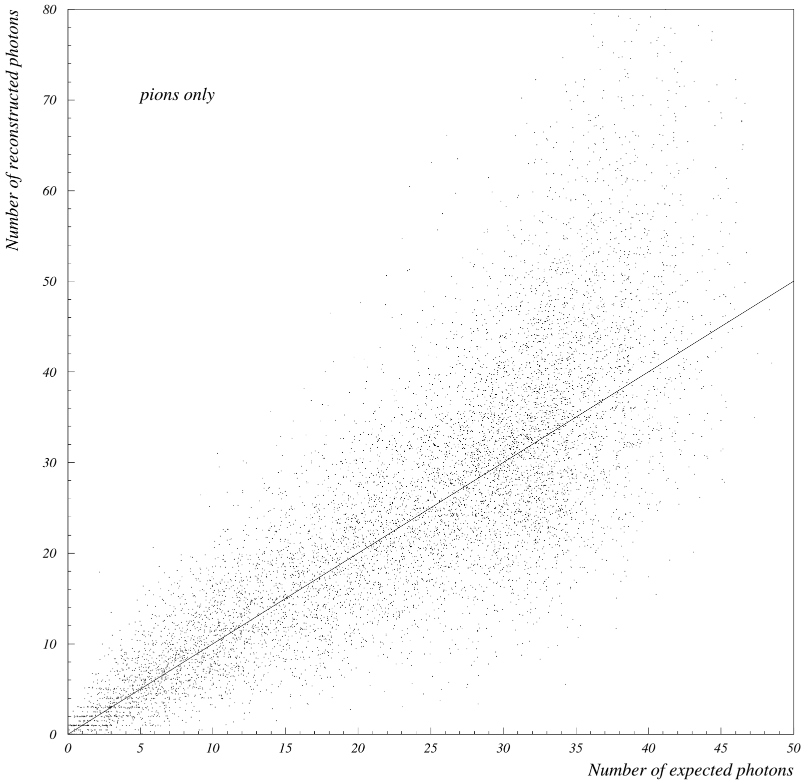

Figure 3: *Number of reconstructed photons, n_r, in the proper hypothesis window after 16 iterations, as compared to the number of expected photons, n_e. Events analyzed were of the type expected in the HERA-B spectrometer. The line corresponds to the case $n_e = n_r$.*

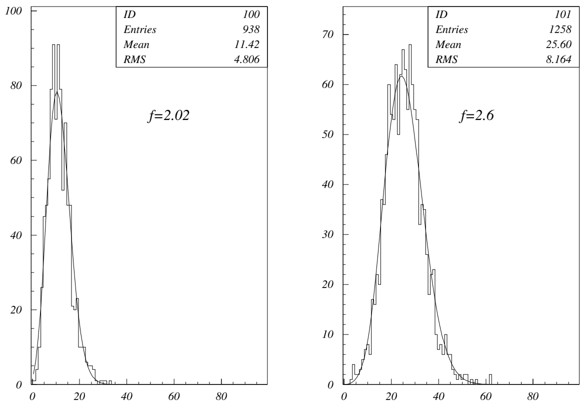

Figure 4: *Number of reconstructed photons in the proper hypothesis window after 16 iterations, for 10 expected photons (left) and 25 expected photons (right). The curves correspond to a Poissonian-like distribution Eq. 1, with the value of factor f (Eq. 2) indicated for each case.*

specific example displayed in Fig. 4 one expects an r.m.s. of 5 photons if 25 photons are detected on average, and the observed value is 6.3. To model the distribution, we replaced the Possion distribution of the number of reconstructed photons n_r with mean $\bar{n}_r$, $P(\bar{n}_r, n_r)$, with a Poisson-like function

$$P'(n_e, n_r) = P(\frac{\bar{n}_r}{f}, \frac{n_r}{f}), \tag{1}$$

where the factor f is determined from the r.m.s width and mean of the distribution,

$$f = \sigma^2_{n_r}/\bar{n}_r. \tag{2}$$

As can be seen from Fig. 4, the function defined in such a way describes the observed distributions reasonably well. The value of f was calculated for each interval of $\bar{n}_r$, and was later used in a tabular form in the likelihood analysis of data.

The effect of a uniformly distributed background was studied as well. On top of the pattern in Fig. 1 we have uniformly distributed 300 hits in the region shown in Fig. 5. The corresponding initial histrogram for the track 1 of Fig. 2 can be seen in Fig. 6, together with the result after 16 iterations. If compared to the result in case of no uniform background (Fig. 2), the reduction of background is still very efficient, although less than in the case without uniform background.

3 Likelihood function

The likelihood function is constructed in the following way. We first denote by $F(\theta, \theta^{hyp})$ the probability density function of detected photons in the Čerenkov angle, calculated for a specific track under the assumption of the track mass hypothesis *hyp*,

$$F(\theta, \theta^{hyp}) = p\ S(\theta, \theta^{hyp}) + (1-p)\ B(\theta, \theta^{hyp}), \tag{3}$$

where S and B are the probability density functions corresponding to the signal and background, respectively, and p is the ratio of the expected numbers of signal and background hits,

$$p = \frac{n_e^s}{n_e^s + n_e^b}.$$

The extended likelihood function [1] now reads

$$\log L^{hyp} = \sum \log F(\theta_i, \theta^{hyp}) + \log P(n_e, n_r), \tag{4}$$

where the number of signal photons is assumed to be distributed according to the Poisson distribution $P(n_e, n_r)$ with mean n_e. As discussed in the previous section, however, we have to account for the somewhat larger variations in the number of reconstructed photons, as observed in Fig. 4, and documented in Eq. 1. Also, we have to consider each photon i in a given histogram with the corresponding weight w_i. Instead of the above expression we therefore use the function

$$\log L^{hyp} = \sum w_i \log F(\theta_i, \theta^{hyp}) + f \log P'(n_e, n_r), \tag{5}$$

where the index i runs over all photons in the $\pi/K/p$ hypotheses windows.

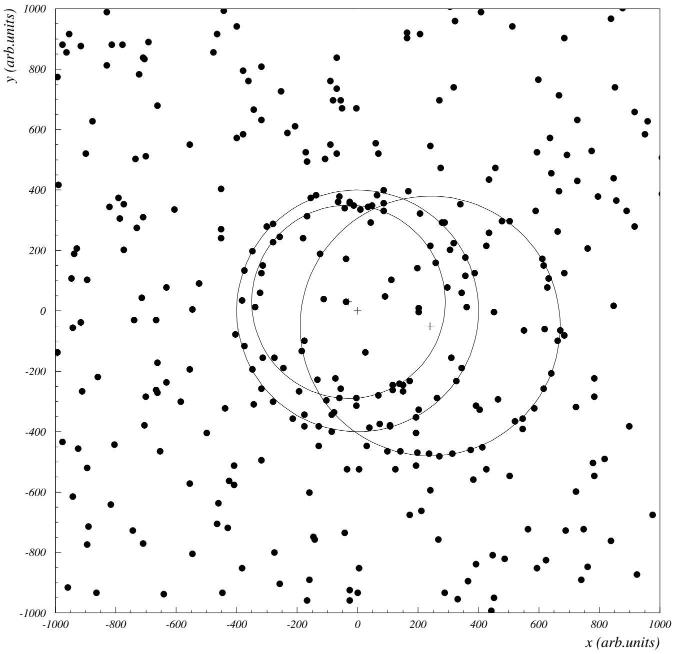

Figure 5: *Three overlapping Čerenkov rings of the test example, with a uniform background superimposed.*

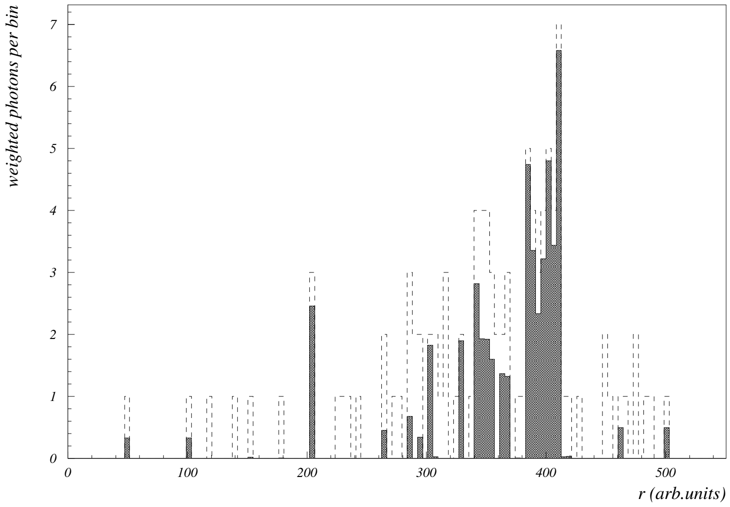

Figure 6: *Photon hit histogram for one of the tracks in Fig. 5 in the case of a superimposed uniformly distributed background, before (dashed line) and after (full histogram) 16 iterations.*

4 K/π separation in the HERA-B RICH

To demonstrate the efficiency of the method, we will consider a particular example of the RICH counter in the HERA-B experiment. The HERA-B detector at the HERA e-p collider at DESY in Hamburg aims at measuring CP violation parameters in the B-meson system using thin-strip, fixed targets in the halo of the 820 GeV proton beam [2, 3]. B mesons will be thus produced in proton-nucleus collisions and their decays to J/ψ + K_s^0 will be measured. Tagging of the B meson flavour will be performed by identification of the charged kaon into which the associated B meson decayed. For this purpose a RICH counter will be used [4]. The RICH detector will consist of 2.7 m of perfluorobutane (C_4F_{10}) gas radiator, spherical mirrors of 5.75 m focal length and about 6 m^2 of photon detectors with a pixel size of 9x9 mm^2 and 18x18 mm^2, matching the required resolution and expected hit occupancy and the required resolution.

To illustrate the environment, we plot in Fig. 7 the expected occupancy on the photon detector, and a typical event. Events were generated by the GEANT program [5]. Charged tracks were tracked through the radiator. Čerenkov photons were generated and followed to the photon detector. Since the main contribution to the background in this particular RICH detector arises from Čerenkov photons emitted by charged particles coming from the same event, the method discussed in this paper should be advantageous.

In the analysis of the simulated RICH data all detected photons were taken into consideration for each track within an event, and the iteration algorithm was repeated twenty times. The shape of the background was determined from the Čerenkov angle histograms after the last iteration, and turned out to be well described by a cubic function in Čerenkov angle θ.

We note that in order to minimize the influence of the background shape on the identification, only photons within $\pm 3\sigma_\theta$ around each of the possible particle hypotheses are taken into account when calculating the log-likelihood function. We also note that for pion, kaons and protons we have not considered hypotheses that can be excluded by using information from other detector components (electrons and muons). For electrons and muons, in turn, only the electron or muon window was considered, respectively.

5 Results

The pion-kaon separation is shown in Fig. 8, where the logarithm of the ratio of likelihoods $\log L^\pi/L^K$ is plotted against the particle momentum. Of course, the efficiency and fake probability depend on the cuts in the likelihood ratio applied to separate pions from kaons. By fixing the pion fake probability to a certain value a momentum dependent cut on the likelihood ratio is defined. In Fig. 9 the efficiency of the method is shown for a fixed pion fake probability of 5%.

It is interesting to compare the result with the performance of the usual method, in which the likelihood functions are calculated without the iteration procedure. As can be seen from the Fig. 9, the method described in this paper certainly improves the performance of the RICH counter.

References

[1] P. Baillon, Nucl. Instr. Meth. **238**(1985)341.

[2] T. Lohse et al. *Proposal for HERA-B*, DESY PRC-94/02, May 1994

[3] P.Križan, R. Mankel, D. Ressing, S. Shuvalov, M. Spahn, Nucl. Instr. Meth. **A351**(1994)111

[4] P. Križan et al., Nucl. Instr. Meth. **A371**(1996)151

[5] S. Nowak, H B GEAN, HERA-B Note94-123.

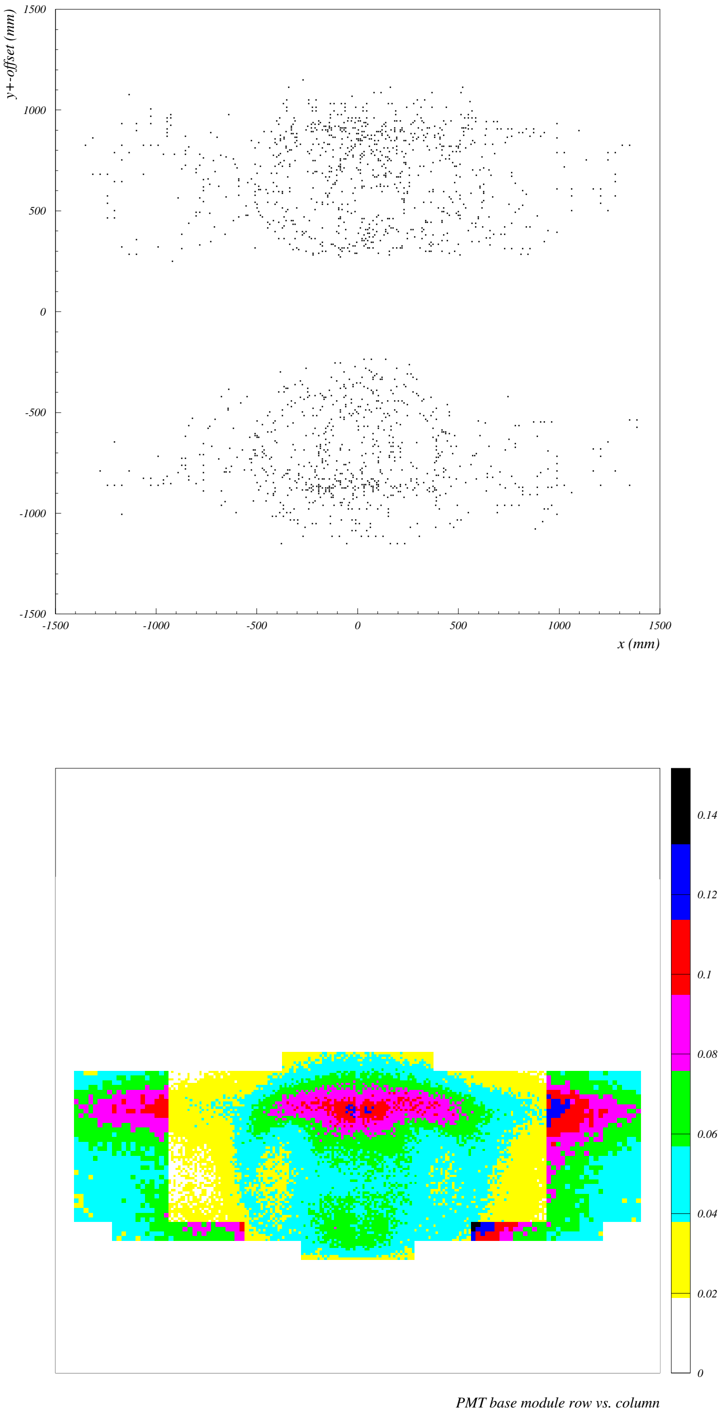

Figure 7: *The HERA-B RICH. Top: a typical event expected in the HERA-B RICH counter. Bottom: the occupancy per channel on the upper half of the photon detector. A sharp change can be observed at the boundary between the inner, finer granularity, and the outer, coarser granularity part.*

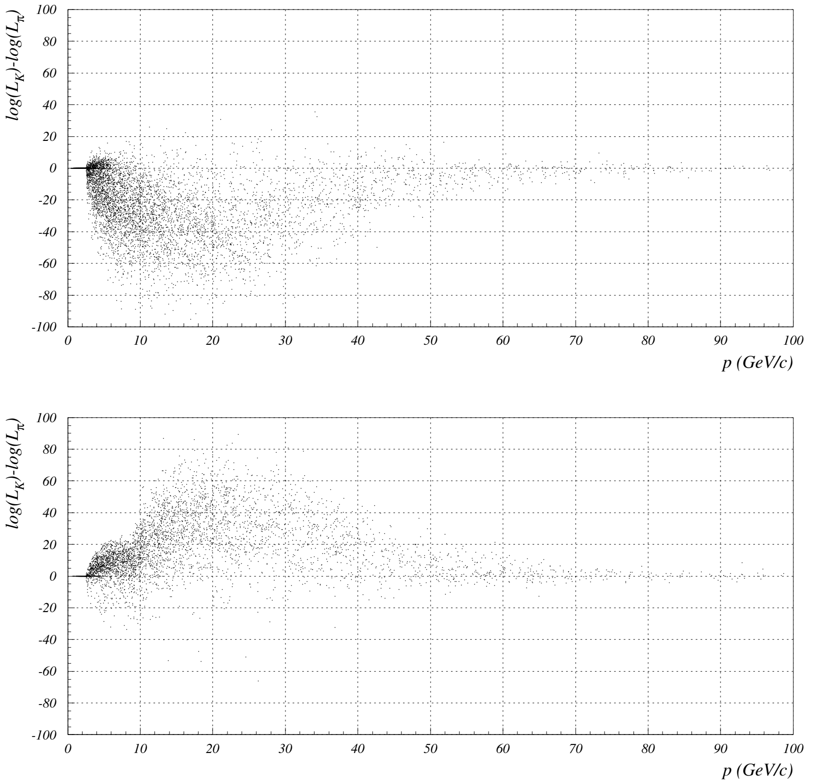

Figure 8: *The log-likelihood difference of the kaon and pion hypotheses for pions (above) and kaons (below), as a function of momentum. It was assumed that on average 30 photons are detected per* $\beta = 1$ *charged particle, and that a single photon determines the Čerenkov angle with* $\sigma_\theta = 0.6\ 10^{-3}$.

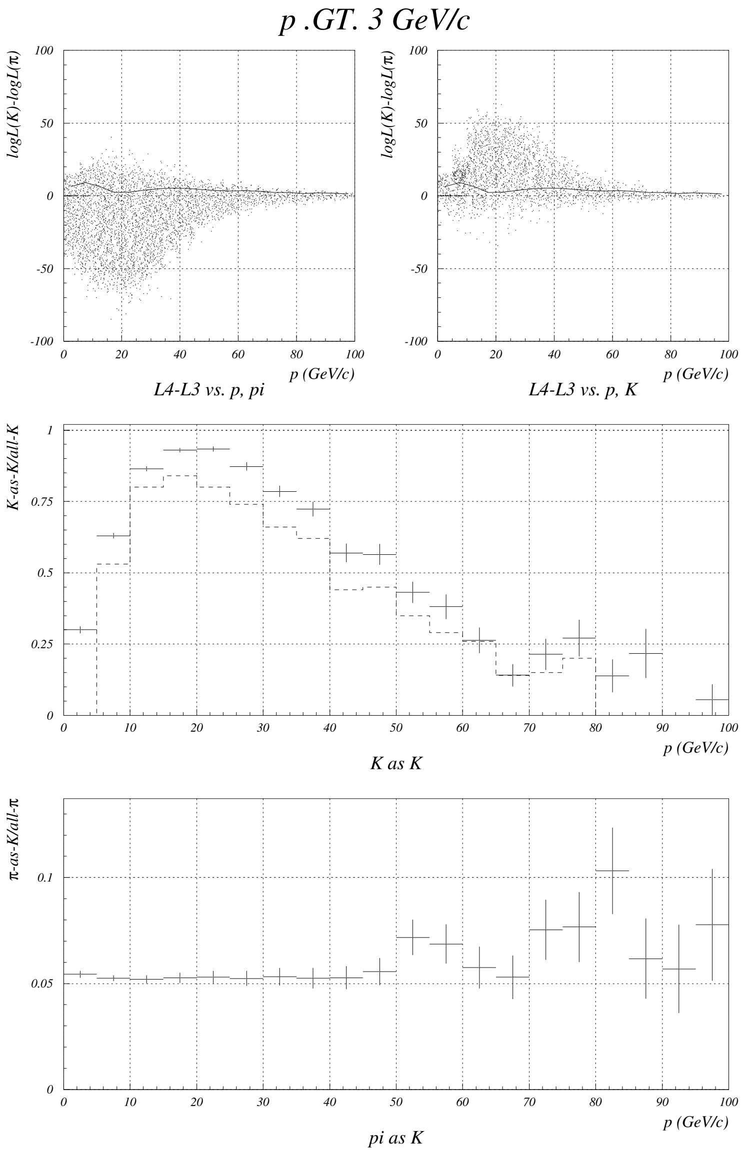

Figure 9: *The momentum dependent efficiency for resolving a kaon from a pion (plot in the middle), extracted from Fig. 8 under the requirement that the probability for a pion to be identified as a kaon (lower plot) amounts to 5%. The corresponding cut in the log-likelihood difference is shown in the upper two plots. For comparison, we show as a dashed histogram the efficiency of the pion-kaon separation without performing the iteration procedure.*